Reviews on Advanced Materials and Technologies, 2024, vol. 6, no. 4, pp. 178–182
DOI: 10.17586/2687-0568-2024-6-4-178-182

Electrical Characteristics and Peculiarities of Formation of Type II InAsSb/InAsSbP Heterostructures

I.D. Kirilenko[1,*], M.S. Ruzhevich[1], N.L. Bazhenov[2], M.V. Tomkovich[2], V.V. Romanov[2], K.D. Moiseev[2], K.D. Mynbaev[1,2]

[1] Institute of Advanced Data Transfer, ITMO University, 49 Kronverkskiy, Saint-Petersburg 197101
[2] Ioffe Institute, 26 Polytechnicheskaya, Saint-Petersburg 194021

Article history

Received November 22, 2024
Accepted November 25, 2024
Available online December 30, 2024

Abstract

This article presents the results of a study of current-voltage (*I–V*) characteristics of InAsSb/InAsSbP heterostructures with an InSb content in the InAsSb active region 0.06 and 0.09. Using these results, the results of electroluminescence studies, and the data of energy-dispersive X-ray spectroscopy obtained for InAsSbP films grown on InAs(Sb), it is shown that the peculiarities of formation of the InAsSb/InAsSbP heterointerface via the method of metalorganic vapor phase epitaxy can lead to the development of a type II heterojunction. At temperatures $T \leq 170$ K, this is manifested in specific values of both the energy of electroluminescence spectrum maximum and the *I–V* cutoff value.

Keywords: Solid solutions; InAsSbP; Electroluminescence; Heterostructures

1. INTRODUCTION

InAsSb-based light-emitting diodes (LEDs) are widely used in optoelectronic devices operating in the middle-wave infrared range of the spectrum (wavelengths 3–6 μm) [1–3]. The simplest and the most common design of heterostructures (HSs) for these LEDs is the one where an active region made of *n*-InAsSb is enclosed between an *n*-InAs or *n*-GaSb substrate and a *p*-InAsSbP barrier layer. Carrier recombination in these HSs is normally expected to proceed in the active region near the *n-p* heterointerface. In practice, however, the LED photon energy does not always correspond to the bandgap E_g of the active region, especially at low temperatures [4,5]. The reason for that is the dominance of recombination mechanisms other than interband, such as interface and/or impurity-related [4–6] ones, due to the peculiarities of the formation of the InAsSb/InAsSbP heterointerface. These are determined by the mismatch of the crystal lattice parameters of InAsSb and InAsSbP, and the specifics of the deposition of InAsSbP on InAsSb by metal-organic vapor phase epitaxy (MOVPE). These factors can lead to a considerable deviation of the chemical composition of the barrier layer from the nominal one (calculated for the growth procedure) [5–7]. Considering these factors is important when developing HSs for LEDs. In this paper, we present the results of the study of electrical characteristics of InAsSb-based HSs and assess the influence of the properties of InAsSbP barrier layers on these characteristics. To this end, properties of HSs and those of epitaxial InAsSbP films deposited on InAs(Sb) were studied.

* Corresponding author: I.D. Kirilenko, e-mail: idkirilenko@itmo.ru

© 2024 ITMO University. This is an open access article under the terms of the CC BY-NC 4.0 license.

2. MATERIALS AND METHODS

Epitaxial films and HSs were grown in a horizontal reactor at atmospheric pressure [8]. Undoped (001)InAs wafers with the electron concentration $n = 3\cdot10^{16}$ cm^{-3} (measured at the temperature $T = 300$ K) were used as substrates. The active region of HSs with the thickness ~ 3 μm represented an epitaxial layer of $InAs_{1-y_1}Sb_{y_1}$ with $y_1 = 0.06$ or $y_1 = 0.09$ and was not intentionally doped. $InAs_{1-x-y_2}Sb_{y_2}P_x$ barrier layers were 1.2 μm thick and had *p*–type conductivity obtained by doping them with zinc during the growth.

On the basis of the HSs, LED chips were manufactured and mounted on TO-18-type housings. Current-voltage (*I–V*) characteristics of the HSs were recorded in $T = 4.2$–300 K range with a step $\Delta T = 5$ K using a PCSU1000 electronic two-channel oscilloscope connected to a personal computer. An electric circuit containing a sinusoidal voltage generator (frequency 100 Hz) was used. To measure the current, 1 Ohm load resistor was connected in series with the chip. Chemical composition of InAsSbP films was studied with energy-dispersive X-ray spectroscopy (EDX) using FEI Quanta 200 electron microscope.

3. RESULTS AND DISCUSSION

To understand the challenges we address, let us first briefly review the results of the studies of electroluminescence (EL) of the HSs. EL spectra were presented and discussed elsewhere [4,5]; they were recorded using an MDR-23 grating monochromator and a cooled InSb-based photodiode under pulsed excitation with a frequency 1 kHz and pulse duration 2 μs. At low temperatures, the spectra contained two bands. The high-energy band centered at ~ 0.41 eV at $T = 4.2$ K was related to carrier recombination in the InAs substrate near the InAs/InAsSb heterointerface. The low-energy bands centered at 0.335 eV and 0.311 eV at $T = 4.2$ K for HSs with $y_1 = 0.06$ and $y_1 = 0.09$, respectively, were related to recombination at the InAsSb/InAsSbP heterointerfaces. Symbols *1* and *2* in Fig. 1 show temperature dependencies of the low-energy band maxima and those of calculated (according to [8]) values of E_g of the active region for the studied HSs with $y_1 = 0.06$ and $y_1 = 0.09$, respectively. It can be seen that the energy of the maxima E_{EL} is close to E_g at high temperatures, yet with the temperature decreasing, starting from $T \approx 150$ K, E_{EL} becomes smaller than E_g. The difference between E_g and E_{EL} at $T \approx 4.2$ K is equal ~ 28 meV and ~ 36 meV for HSs with $y_1 = 0.06$ and $y_1 = 0.09$, respectively.

The temperature dependences of E_{EL} shown by symbols *1* and *2* in Fig. 1 for the studied HSs differed significantly

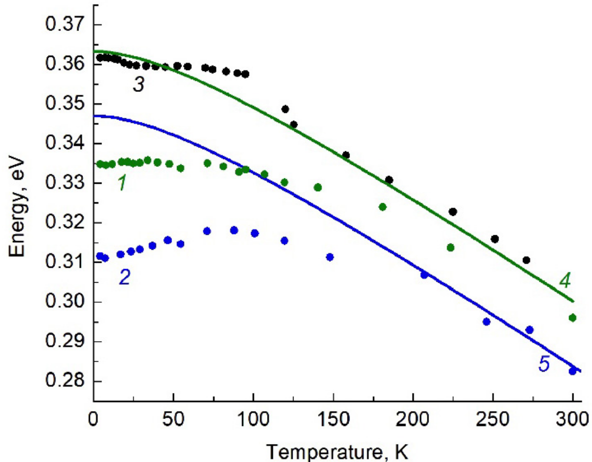

Fig. 1. A review of $E_{EL}(T)$ dependencies for the $InAs_{1-y_1}Sb_{y_1}$/InAsSbP HSs with $y_1 = 0.06$ (symbols *1*) and $y_1 = 0.09$ (*2*) (replotted from Ref. [5]), and with $y_1 = 0.06$ (from Ref. [10]) (*3*); curves *4* and *5* show calculated $E_g(T)$ for $InAs_{1-y_1}Sb_{y_1}$ with $y_1 = 0.06$ and $y_1 = 0.09$, respectively.

from that for a HS with an active region with similar value of y_1 grown using a low-pressure MOVPE technology described in Ref. [9]. For the latter, as shown in Fig. 1 by symbols *3*, the E_{EL} values were always close to the calculated values of E_g, except for $T < 100$ K, where stimulated emission was observed from the HS [10].

It appeared that the features of the HSs studied in this work showed not only in their EL spectra, but also in the electrical properties. Fig. 2a shows *I–V* characteristics for the HS with $y_1 = 0.09$, recorded at various temperatures. One can see a decrease in the slope of the forward branch with temperature increasing, as well as a decrease in the forward cutoff value V_{co}. Fig. 2b shows the temperature dependences of V_{co} for both HSs studied in this work, and, for comparison, a similar dependence from [11] for the HS with $y_1 = 0.06$, whose optical properties were presented in Ref. [10]. As can be seen in Fig. 2b, in the latter case the V_{co} increased linearly with T decreasing. For the HSs studied in this work, the behavior of V_{co} was somewhat different. When the temperature was lowered from the room temperature to $T \approx 150$ K, the nature of the change in V_{co} was close to that for the HS from Ref. [11], but with a further decrease in temperature V_{co} grew faster. At $T = 4.2$ K, for HSs with the same $y_1 = 0.06$, yet manufactured using different technologies, a difference of $\Delta V_{co} \approx 150$ meV was observed.

In order to understand the reasons for the experimentally observed features of the optical and electrical characteristics of the studied HSs, it is necessary to consider their energy band diagrams. Let us note that since the resulting carrier concentration in the barrier layer ($p = 5\ 10^{17}$ cm^{-3}) exceeds the concentration of the majority carriers in the active region by an order of magnitude, the entire contact

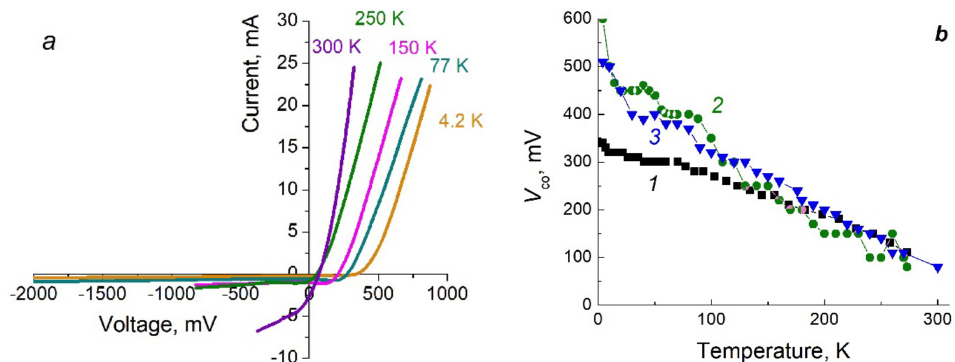

Fig. 2 (a) *I–V* characteristics for the $InAs_{1-y_1}Sb_{y_1}$/InAsSbP HS with $y_1 = 0.09$ recorded at various temperatures; (b) dependencies of V_{co} on the temperature: for the HS with $y_1 = 0.06$ from Ref. [11] (*1*), and for HSs studied in this work with $y_1 = 0.06$ (*2*) and $y_1 = 0.09$ (*3*).

potential difference falls on the active layer, where the space charge region is also located. The structures in Refs. [10,11] were type I heterojunctions, which was in good agreement with the results of the electrical and optical studies. For the heterojunctions studied in this work, the calculation of the band diagrams based on the nominal (calculated for the growth) values of the $InAs_{1-x-y_2}Sb_{y_2}P_x$ barrier layer composition ($y_2 = 0.22$, $x = 0.47$) also suggested formation of a type I heterojunction. However, the above-mentioned peculiarities of the formation of the InAsSbP layer by the atmospheric-pressure MOVPE at the InAsSb surface can lead to a deviation of the actual composition of InAsSbP from that specified in the pre-growth calculations and, thus, to changes in the energy band diagram due to variations in the bandgap of InAsSbP.

To study this effect, we assessed E_g of the InAsSbP barrier layers via an EDX study of chemical composition of InAsSbP films grown on $InAs_{1-y_1}Sb_{y_1}$ with different y_1. Accelerating voltage 10 kV was used and analyzed were InAsSbP epitaxial films grown on InAsSb with y_1 ranging from 0 to 0.16. The thickness of the analyzed layer was calculated using CASINO® software [12], and equaled 400 nm. The EDX data showed that the increase in the InSb content y_1 in the $InAs_{1-y_1}Sb_{y_1}$ indeed increases InSb content y_2 in $InAs_{1-x-y_2}Sb_{y_2}P_x$, while concentrations of P (i.e., x) and As decrease. Fig. 3 shows a dependence of the value of E_g of the InAsSbP quaternary solid solution calculated for $T = 300$ K on the basis of the EDX data according to the formula presented in Ref. [13]. Values of E_g for InAs, InSb and InP were taken as 0.354, 0.175 and 1.344 eV, respectively, while bowing parameters C for InAsP, InAsSb and InSbP were taken as 0.20, 0.61 and 1.83 eV, respectively [7]. For comparison, photoluminescence (PL) data (energies of PL peaks at 300 K) are also shown in Fig. 4, from Refs. [6,14] and from our own experiments. Details of the latter will be presented elsewhere; they were performed using a set-up described in Ref. [15], which was similar to that used in Ref. [14]. As can be seen, both EDX and PL data show gradual, almost linear decrease in the bandgap of the InAsSbP barrier layer with the InSb content in the active layer increasing up to $y_1 = 0.12$.

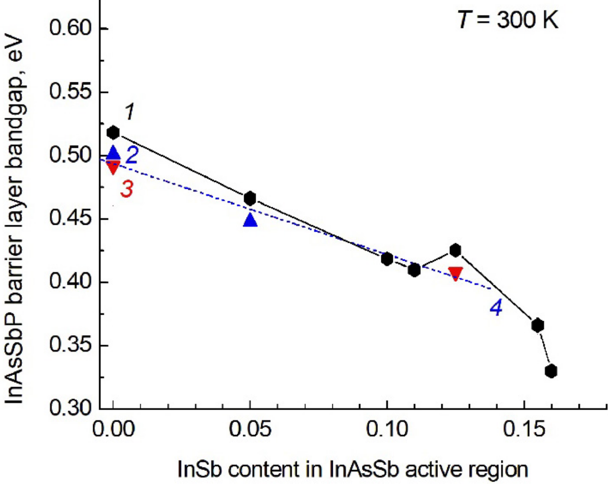

Fig. 3. The dependence of the bandgap of the InAsSbP layer on the InSb content in the underlying InAs(Sb) 'substrate': EDX data (*1*) and PL data from Ref. [14] (*2*) and from this work (*3*); line *4* shows linear approximation of the PL data.

Using the data obtained with EDX, PL, and those of secondary-ion mass spectroscopy (SIMS) from Ref. [6], calculations of the composition of InAsSbP barrier layers in the studied HSs were performed. For the growth on $InAs_{1-y_1}Sb_{y_1}$ with $y_1 = 0.06$ and $y_1 = 0.09$, calculations for $InAs_{1-x-y_2}Sb_{y_2}P_x$ yielded $y_2 = 0.25$, $x = 0.44$, and $y_2 = 0.26$, $x = 0.42$, respectively. Fig. 4 shows the energy band diagrams of the studied HSs, constructed at $T = 77$ K for both nominal (for $y_1 = 0.06$ only, Fig. 4a,d) and calculated (factual) (Fig. 4b,c,e,f) values of y_2 and x. Carrier concentration in the active region was taken as $n = 5\ 10^{16}$ cm^{-3}. It is evident that with the actual compositions of the barrier layer, a type II InAsSb/InAsSbP heterojunction is formed (Fig. 4b,c). At thermodynamic equilibrium (see Fig. 4b,c) there is a potential barrier for holes, but when a forward bias is applied, in the type I structure the barrier almost disappears and the holes can easily penetrate into the

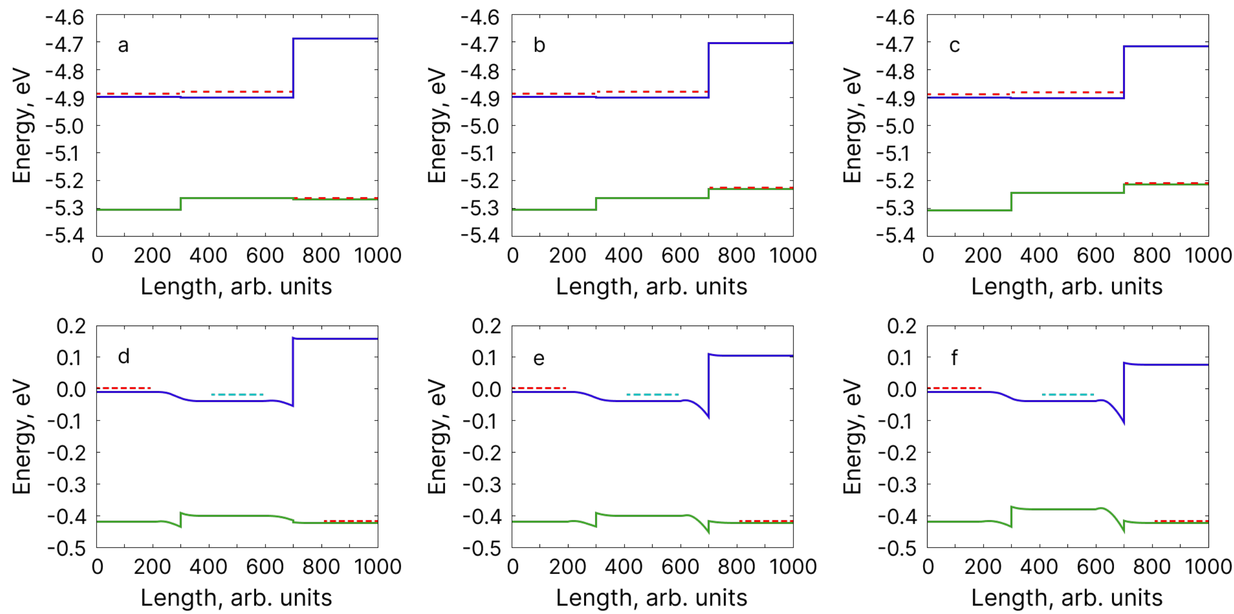

Fig. 4. Band diagrams at $T = 77$ K for n-InAs/InAs$_{1-y_1}$Sb$_{y_1}$/p-InAs$_{1-x-y_2}$Sb$_{y_2}$P$_x$ HSs: (a,d) with $y_1 = 0.06$, $y_2 = 0.22$, $x = 0.47$; (b,e) with $y_1 = 0.06$, $y_2 = 0.25$, $x = 0.44$; (c,f) with $y_1 = 0.09$, $y_2 = 0.26$, $x = 0.42$; (a,b,c) at equilibrium; (d,e,f) at forward bias $U_{for} \sim 400$ mV.

active layer (Fig. 4d). In the HS of the type II, however, a barrier equal to the band offset is retained (~ 30 meV, Fig. 4e,f), and this hinders the transport of holes, especially at low temperatures, when their thermal energy decreases. Also, in the HS of the type II, a deep potential well for electrons forms in the conduction band. As a result, recombination takes place between the electrons localized in this well and the holes retained by the barrier at the heterointerface (see, e.g., Ref. [6]). As a result, the photon energy turns out to be significantly lower than E_g of the active region, while the existence of additional energy barriers affects the cutoff of the *I*–*V* characteristic.

The factors listed above explain the difference in the *I*–*V* characteristic and the temperature dependence of E_{EL} for InAsSb/InAsSbP HSs of type I and II with the same antimony content in the InAsSb active region observed at low temperatures. With increasing temperature, carriers are delocalized due to their thermalization, and carrier recombination in HSs of both type I and type II takes place in the active region. The cutoffs in the direct branches of the *I*-*V* characteristics also become close. Thus, the features of the optical and electrical characteristics of InAsSb/InAsSbP HSs of type II appear only at low temperatures ($T \leq 150$ K).

4. CONCLUSION

A variable-temperature ($T = 4.2$–300 K) study of *I*–*V* characteristics of n-InAs/n-InAs$_{1-y_1}$Sb$_{y_1}$/p-InAsSbP LED heterostructures with $y_1 = 0.06$ and $y_1 = 0.09$ was performed to complement electroluminescence (EL) studies carried out earlier. It was found that peculiarities in both cut-offs of the *I*–*V* characteristics and the position of the EL spectra at low temperatures ($T \leq 150$ K) were caused by formation of a type II InAsSb/InAsSbP heterojunction. This was confirmed with the results of EDX studies performed on InAsSbP films grown on InAs$_{1-y_1}$Sb$_{y_1}$ material with $y_1 = 0\ldots0.16$. At high temperatures, the EL spectra and *I*–*V* characteristics of InAsSb/InAsSbP heterostructures of types I and II appear to become indistinguishable. In this regard, a comparative analysis of the quantum efficiency of type I and II heterostructures with a similar composition of the active region is of interest, since the influence of the properties of the heterointerface can be a factor in efficiency value. Such an analysis should be the subject of further research.

ACKNOWLEDGMENTS

The authors would like to thank Dr. D.D. Firsov and I.V. Chumanov for performing photoluminescence measurements.

REFERENCES

[1] G.F. Rangel, L.D. de Leon Martínez, L.S. Walter, B. Mizaikoff, Recent advances and trends in mid-infrared chem/bio sensors, *TrAC Trends Analyt. Chem.*, 2024, vol. 180, art. no. 117916.

[2] M. Hlavatsch, B. Mizaikof, Advanced mid-infrared lightsources above and beyond lasers and their analytical utility, *Analyt. Sci.*, 2022, vol. 38, pp. 1125–1139.

[3] D. Jung, S. Bank, M.L. Lee, D. Wasserman, Next-generation mid-infrared sources, *J. Opt.*, 2017, vol. 19, art. no. 123001.

[4] M.S. Ruzhevich, Investigation of Radiation Recombination Channels in Long-Wavelength InAs/InAsSb/InAsSbP LED Heterostructures, Rev. Adv. Mater. Sci. Technol., 2021, vol. 3, no. 4, pp. 24–28.

[5] M.S. Ruzhevich, K.D. Mynbaev, N.L. Bazhenov, V.V. Romanov, K.D. Moiseev, Electroluminescence of narrow-gap $InAs/InAs_{1-y}Sb_y/InAsSbP$ heterostructures with y=0.07–0.12, *St. Petersburg State Polytechnical University Journal. Physics and Mathematics*, 2024, vol. 17, no. 1.1, pp. 77–82.

[6] V.V. Romanov, K.D. Moiseev, Features of the Energy Band Structure of the InAsSbP Epilayer Deposited on a Surface of the $InAs_{1-y}Sb_y$ Solid Solution, *Phys. Solid State*, 2023, vol. 65, no. 10, pp. 1634–1641.

[7] K.D. Moiseev, V.V. Romanov, Band Diagram of the $InAs_{1-y}Sb_y$/InAsSbP Heterojunction in the Composition Range $y < 0.2$, *Phys. Solid State*, 2021, vol. 63, no. 4, pp. 595–602.

[8] V.V. Romanov, E.V. Ivanov, K.D. Moiseev, $InAs_{(1-y)}Sb_y$/InAsSbP Narrow-Gap Heterostructures (y = 0.09–0.16) Grown by Metalorganic Vapor Phase Epitaxy for the Spectral Range of 4–6 μm, *Phys. Sol. State*, 2019, vol. 61, no. 10, pp. 1699–1706.

[9] M. Sopanen, T. Koljonen, H. Lipsanen, T. Tuomi, Growth of GaInAsSb using tertiarybutylarsine as arsenic source, *J. Cryst. Growth*, 1994, vol. 145, no. 1–4, pp. 392–497.

[10] K.D. Mynbaev, N.L. Bazhenov, A.A. Semakova, A.V. Chernyaev, S.S. Kizhaev, N.D. Stoyanov, V.E. Bougrov, H. Lipsanen, Kh.M. Salikhov, Spontaneous and stimulated emission in InAsSb-based LED heterostructures, *Infr. Phys. Technol.*, 2017, vol. 85, pp. 246–250.

[11] A.A. Semakova, N.L. Bazhenov, K.D. Mynbaev, A.V. Chernyaev, S.S. Kizhaev, N.D. Stoyanov, Study of the Current–Voltage Characteristics of InAsSb-Based LED Heterostructures in the 4.2–300 K Temperature Range, *Semiconductors*, 2021, vol. 55, no. 6, pp. 557–561.

[12] D. Drouin, A.R. Couture, D. Joly, X. Tastet, V. Aimez, R. Gauvin, CASINO V2.42 — A Fast and Easy-to-use Modeling Tool for Scanning Electron Microscopy and Microanalysis Users, *Scanning*, 2007, vol. 29, pp. 92–101.

[13] V.V. Romanov, E.V. Ivanov, K.D. Moiseev, Forming a Type-II Heterojunction in the InAsSb/InAsSbP Semiconductor Structure, *Phys. Solid State*, 2020, vol. 62, no. 11, pp. 2039–2044.

[14] T. Smołka, M. Motyka, V.V. Romanov, K.D. Moiseev, Photoluminescence Spectroscopy of the InAsSb-Based *p-i-n* Heterostructure, *Materials*, 2022, vol. 15, no. 4, art. no. 1419.

[15] D.D. Firsov, O.S. Komkov, V.A. Solov'ev, P.S. Kop'ev, S.V. Ivanov, Temperature-dependent photoluminescence of InSb/InAs nanostructures with InSb thickness in the above-monolayer range, *J. Phys. D: Appl. Phys.*, 2016, vol. 49, no. 28, art. no. 285108.

УДК 538.91

Электрические характеристики и особенности формирования гетероструктур II типа InAsSb/InAsSbP

Я.Д. Кириленко[1], М.С. Ружевич[1], Н.Л. Баженов[2], М.В. Томкович[2], В.В. Романов[2], К.Д. Моисеев[2], К.Д. Мынбаев[1,2]

[1] Институт перспективных систем передачи данных, Университет ИТМО, Кронверкский пр., д. 49, Санкт-Петербург 197101
[2] Физико-технический институт им. А.Ф. Иоффе, Политехническая ул., д. 26, Санкт-Петербург 194021

Аннотация. В статье представлены результаты исследования вольт-амперных характеристик (ВАХ) гетероструктур InAs/InAsSb/InAsSbP с содержанием InSb в активной области InAsSb 0.06 и 0.09. С использованием этих результатов, результатов электролюминесцентных исследований и данных энергодисперсионной рентгеновской спектроскопии, полученных на пленках InAsSbP, выращенных на InAs(Sb), показано, что особенности формирования гетерограницы InAsSb/InAsSbP в методе газофазной эпитаксии из металлоорганических соединений могут приводить к формированию гетероперехода II типа. При температурах $T \leq 150$ К это проявляется в специфических значениях энергии максимума спектра электролюминесценции и величины отсечки ВАХ.

Ключевые слова: твердые растворы; InAsSbP; электролюминесценция; гетероструктуры